

Both ATP Sites of Human P-Glycoprotein Are Essential but Not Symmetric[†]Christine A. Hrycyna,[‡] Muralidhara Ramachandra,^{§,||} Ursula A. Germann,^{‡,⊥} Priscilla Wu Cheng,^{‡,∇} Ira Pastan,[§] and Michael M. Gottesman^{*,‡}*Laboratories of Cell Biology and Molecular Biology, Division of Basic Sciences, National Cancer Institute, National Institutes of Health, Bethesda, Maryland 20892**Received May 14, 1999; Revised Manuscript Received July 20, 1999*

ABSTRACT: Human P-glycoprotein (P-gp) is a cell surface drug efflux pump that contains two nucleotide binding domains (NBDs). Mutations were made in each of the Walker B consensus motifs of the NBDs at positions D555N and D1200N, thought to be involved in Mg²⁺ binding. Although the mutant and wild-type P-gps were expressed equivalently at the cell surface and bound the drug analogue [¹²⁵I]iodoarylazidoprazosin ([¹²⁵I]IAAP) comparably, neither of the mutant proteins was able to transport fluorescent substrates nor had detectable basal nor drug-stimulated ATPase activities. The wild-type and D1200N P-gps were labeled comparably with [α-³²P]-8-azido-ATP at a subsaturating concentration of 2.5 μM, whereas labeling of the D555N mutant was severely impaired. Mild trypsin digestion, to cleave the protein into two halves, demonstrated that the N-half of the wild-type and D1200N proteins was labeled preferentially with [α-³²P]-8-azido-ATP. [α-³²P]-8-Azido-ATP labeling at 4 °C was inhibited in a concentration-dependent manner by ATP with half-maximal inhibition at approximately 10–20 μM for the P-gp-D1200N mutant and wild-type P-gp. A chimeric protein containing two N-half NBDs was found to be functional for transport and was also asymmetric with respect to [α-³²P]-8-azido-ATP labeling, suggesting that the context of the ATP site rather than its exact sequence is an important determinant for ATP binding. By use of [α-³²P]-8-azido-ATP and vanadate trapping, it was determined that the C-half of wild-type P-gp was labeled preferentially under hydrolysis conditions; however, the N-half was still capable of being labeled with [α-³²P]-8-azido-ATP. Neither mutant was labeled under vanadate trapping conditions, indicating loss of ATP hydrolysis activity in the mutants. In confirmation of the lack of ATP hydrolysis, no inhibition of [¹²⁵I]IAAP labeling was observed in the mutants in the presence of vanadate. Taken together, these data suggest that the two NBDs are asymmetric and intimately linked and that a conformational change in the protein may occur upon ATP hydrolysis. Furthermore, these data are consistent with a model in which binding of ATP to one site affects ATP hydrolysis at the second site.

One of the major obstacles to effective chemotherapy of cancer is the phenomenon of multidrug resistance. For many years, oncologists have observed that tumors that became resistant to one cytotoxic agent often became resistant to a wide variety of compounds including the vinca alkaloids, anthracyclines, and paclitaxel (1, 2). This broad-based cellular resistance is due, in part, to the expression of an energy-dependent transport protein named P-glycoprotein (P-gp)¹ (3). P-gp is a 170 kDa phosphorylated glycoprotein present in the plasma membrane of many cell types (4).

Human P-glycoprotein is a 1280 amino acid protein encoded by the *MDR1* gene (3). It is composed of two homologous halves, each containing six putative transmembrane domains and one nucleotide binding/utilization domain (NBD) also called the ATP-binding cassette (ABC) (4). The two halves are separated by a 77 amino acid linker peptide that is thought to allow the two halves of P-gp to interact properly in the functional molecule (5). P-gp is an ATPase and utilizes the energy from ATP hydrolysis to reduce the accumulation of drugs or other toxins within cells by acting as a drug efflux pump (1, 2, 6). P-gp also effectively reduces the rate of influx of drugs, suggesting that it acts by removing the compounds from within the lipid bilayer (2).

The minimal functional unit of P-gp, and in fact for all of the known ABC transporters to date, is two NBDs and two membrane domains (7). The NBDs are defined by three consensus motifs. The Walker A nucleotide binding fold consensus sequence is G-(X)₄-G-K-(T/S)-(X)₆-I/V and the

[†] C.A.H. was supported in part by a postdoctoral fellowship from The Jane Coffin Childs Memorial Fund for Medical Research.

* To whom correspondence should be addressed at the Laboratory of Cell Biology, National Cancer Institute, National Institutes of Health, 37 Convent Dr., MSC 4255, Bethesda, MD 20892-4255. Telephone (301) 496-1530; FAX (301) 402-0450; e-mail mgottesman@nih.gov.

[‡] Laboratory of Cell Biology, NCI.

[§] Laboratory of Molecular Biology, NCI.

^{||} Present address: Canji, Inc., 3030 Science Park Rd., San Diego, CA 92121.

[⊥] Present address: Vertex Pharmaceuticals Inc., 130 Waverly St., Cambridge, MA 02139.

[∇] Present address: Department of Dermatology, Johns Hopkins University Medical Center Outpatient Center, 601 North Caroline St., Baltimore, MD 21287.

¹ Abbreviations: ¹P-gp, P-glycoprotein; Vi, sodium orthovanadate; UV, ultraviolet light at 365 nm; [¹²⁵I]IAAP, [¹²⁵I]iodoarylazidoprazosin; [α-³²P]-8-azido-ATP, [α-³²P]-8-azidoadenosine 5'-triphosphate; NBD, nucleotide binding domain; ABC, adenosine triphosphate binding cassette.

Walker B binding fold consensus sequence is R/K-(X)₃-G-(X)₃-L-(hydrophobic)₄-D, where X is any amino acid (8). Additionally, ABC transporters are defined by a third consensus motif called the C-region, signature sequence, or linker dodecapeptide, defined by the consensus sequence LSGGQ (2, 9, 10). This sequence just precedes the Walker B consensus motif and may be involved in substrate recognition or in coupling substrate binding to ATP hydrolysis or in interactions with other domains of the protein (11, 12).

The precise mechanism of action of P-gp has been studied in some detail but is not completely understood (13). Both ATP sites are necessary for activity, as mutations in the Walker A motif of either NBD eliminate or reduce function (14–16). Senior and colleagues (17) demonstrated through chemical means that each ATP site is capable of hydrolyzing ATP and that 1 mole of Mg²⁺-8-azido-ADP is bound per mole of hamster P-gp after hydrolysis (18). Further studies showed that chemical modification of one ATP site prevents hydrolysis at the second site (19). UV-induced vanadate cleavage experiments with human P-gp directly demonstrated that only one hydrolysis event can occur at a time and that the sites are functionally interdependent (20). Disruption of the linker region joining the two halves of the protein eliminates drug transport as well as ATPase activity, even though the ATP sites are intact, suggesting that the two sites interact in some manner (5). The two ATP sites of the cystic fibrosis transmembrane regulator (CFTR) have been shown to have distinguishable activities and properties, suggesting that the two sites may be serving different roles (21). Similar functional asymmetry of the two ATP sites in CED-7 from *Caenorhabditis elegans*, an ABC transporter involved in the engulfment of cell corpses during programmed cell death, has been suggested from mutational analysis (22). However, the exact roles and nature of each of the two ATP sites and the interaction between them in the full-length human P-gp molecule remains unresolved.

In the present study, we explored the nature of the two ATP sites of human P-gp and their interaction. We studied human P-gp chimeric molecules and evaluated the effects of point mutations within the Walker B consensus motifs presumed to be involved in Mg²⁺ binding or coordination. Through analysis of the nucleotide- and drug-binding properties of these molecules as well as transport function and ATPase activity, we determined that the two ATP sites are essential and asymmetric and that the two sites appear to have different accessibilities to nucleotide. Our data suggest that the two sites are intimately linked and that a conformational change in the ATP site or in the entire protein may occur upon nucleotide hydrolysis. These data are consistent with a model in which binding at one ATP site affects hydrolysis at the second site. We provide further evidence that the Walker B mutant P-gps exist in a conformationally distinct form at the cell surface and that this form represents an ATP hydrolysis-incompetent species. Through the exploration of the requirement for magnesium for ATP photoaffinity labeling, it appears that magnesium may be playing an additional role in stabilizing the conformation of the active site or changing the conformation of the overall transporter.

EXPERIMENTAL PROCEDURES

Materials. Dulbecco's modified Eagle's medium (DMEM) with glucose and phenol red was from Quality Biological

(Gaithersburg, MD). Iscove's modified Dulbecco's medium (IMDM), Lipofectin, and trypsin–EDTA were obtained from Life Technologies Inc. (Grand Island, NY). Fetal bovine serum (FBS) was from HyClone (Logan, UT). [¹²⁵I]iodoaryl-azidoprazosin ([¹²⁵I]IAAP) was from NEN DuPont (Boston, MA). [α -³²P]-8-azidoadenosine 5'-triphosphate ([α -³²P]-8-azido-ATP) (100–111 μ M) was from ICN Pharmaceuticals (Irvine, CA). Rhodamine 123 was from Kodak Co. (New Haven, CT). All other chemicals were obtained from Sigma (St. Louis, MO). Enzymes used for recombinant DNA techniques were from New England Biolabs (Beverly, MA).

Vaccinia Virus Expression Vector Constructs: Point Mutations. Specific point mutations were constructed by sequence overlap PCR methodology using pTM1-*MDR1* (wild-type) (23) DNA as the expression vector template. Two internal complementary primers were used, each containing the mutation of interest (G \rightarrow A at position 1663 for D555N). The coding sequence for the D555N mutant primer was 5'-CTCCTGCTGAATGAGGCCAC-3'. These primers were used in conjunction with two outer primers that contained the unique restriction sites for *EcoRI* (coding strand, 5'-AATATTAAGGGAAATTTGGAA-3') and *AatII* (noncoding strand, 5'AAACCAGCGATGACGTCAGCA-3'). Reaction A contained 1 μ M each of the *EcoRI* primer and the noncoding strand mutagenic primer. Reaction B contained 1 μ M each of the *AatII* primer and the coding strand mutagenic primer. The primers and nucleotides were subjected to a 5 min "hot start" at 80 °C and then the PCR reaction was performed with *rTth* DNA polymerase XL (GeneAmp XL PCR Kit, Perkin-Elmer, Foster City, CA) and 10 ng of template. The annealing temperatures for reactions A and B were 53.7 and 55.9 °C, respectively, and extension was allowed to continue for 30 s at 72 °C. A total of 25 cycles was used: 94 °C for 10 s, anneal for 10 s, and extension for 30 s. After cycling, the sample was incubated at 72 °C for an additional 2 min before being cooled to 4 °C. The products of reactions A and B were subsequently used in equimolar amounts as the template for reaction C, which contained the *EcoRI* and *AatII* primers. The PCR reaction was carried out as above except that the annealing temperature was 53.9 °C. The product and the pTM1-*MDR1* parent vector were digested with *EcoRI* and *AatII* and the PCR product was ligated into the vector. The resulting plasmid was called pTM1-*MDR1*-D555N.

The D1200N mutant DNA was constructed similarly with two internal complementary primers, each containing the mutation of interest (G \rightarrow A at position 3598 for D1200N). The coding sequence for the D1200N mutant primer was 5'-ATATTTTGTCTTTGAATGAAG-3'. These primers were used in conjunction with two outer primers that contained unique restriction sites for *NdeI* (coding strand, 5'-AGGAG-CAGAAGTTTGAACATA-3') and *AvaI* (noncoding strand, 5'-AGCAGCCGGATCGTCTGACTTA). The annealing temperature for reaction A containing the forward primer that encodes the *NdeI* site and the reverse mutagenic primer was 54.3 °C. The annealing temperature for reaction B containing the forward mutagenic primer and the reverse primer containing the *AvaI* site was 53.6 °C. The annealing temperature for reaction C containing the two restriction site primers was 54.6 °C. The product of reaction C and the pTM1-*MDR1* parent vector were digested with *NdeI* and *AvaI* and the PCR product was ligated into the vector. The

resulting plasmid was named pTM1-*MDR1*-D1200N. The D555N/D1200N double mutant was constructed exactly like pTM1-*MDR1*-D1200N except that pTM1-*MDR1*-D555N was used as the template for the first PCR reaction. The resulting expression plasmid was named pTM1-*MDR1*-D555N/D1200N.

Construction of the P-gp-1N/1N Chimera. pTM1-*MDR1*-1N/1N was constructed to encode a P-gp molecule that contains two identical N-terminal ATP binding cassettes. To aid in the construction of the original vector pHa*MDR1*-1N/1N, two new restriction sites, *FspI* and *ClaI*, flanking the C-terminal ATP binding domain were introduced into pSXLC, a subcloning pGEM derivative containing the *MDR1* cDNA, by recombinant circle mutagenesis (24). To introduce the *FspI* site, nucleotides 3181–3183 were changed from AAG to CGC, which also resulted in a single amino acid substitution (K1061R). The four amplimers used were 5'-AGGGACTGAGCCTGGAGGTGCGCAAGGGCCA-3' and 5'-AGAGCCAGCGTCTGGCCCTTGCGCACCTCCA-3' to produce the restriction site and 5'-GATGTCCGGTCCGGTGGGAT-3' and 5'-GTGGTCCAGCTCCTGGAGCG-3' to complete the recombinant circle. To construct the *ClaI* site, nucleotides 3640, 3643, and 3645 were changed from G, C, and A to A, G, and T, respectively. These changes resulted in two amino acid changes (V1214I and Q1215D). The four oligomers used were 5'-ATACAGAAAGTGAAAAGGT-TATCGATGAAGCCCT-3' and 5'-CTGGCTTTGTCCAGGGCTTCATCGATAACCTTTT-3' to introduce the restriction site and 5'-AGAGCTGACGTGGCTTCATC-3' and 5'-ACAAAGCCAGAGAAGGCCGC-3' to complete the recombinant circle. This vector was named pSXFC.

The DNA fragment encoding the *MDR1* amino ATP-binding cassette was generated by PCR using pSXLC as template and the following primers: forward, 5'-CCT-GAAGGTGCGCAAGGGCAGACGCTGGCCCTG-3' (the underlined sequence is the *FspI* recognition sequence); reverse, 5'-AGAGCCACATCGATAACCTTTTCACTTCTGTGTCCAAGGCT-3' (the underlined sequence is the *ClaI* recognition sequence). The PCR reactions were performed with 100 ng of template DNA and final reagent concentrations of 1 μ M of each primer, 20 mM Tris-HCl, pH 8.2, 10 mM KCl, 6 mM (NH₄)₂SO₄, 2 mM MgCl₂, 1% Triton X-100, 10 ng/mL nuclease-free bovine serum albumin, 200 μ M of each dNTP, and 2.5 units of *Pfu* DNA polymerase (Stratagene, La Jolla, CA). Reactions were overlaid with three drops of mineral oil and cycled 30 times as follows: 94 °C for 1 min, annealing at 42 °C for 2 min, and extension at 75 °C for 2 min. Extension at 72 °C for 7 min followed the final cycle, and the reactions were subsequently stored at 4 °C and purified. The generated fragments were digested with *FspI* and *ClaI* and subcloned into pSXFC. Since pSXFC contained a *FspI* site, the vector was initially digested with *HindIII* and *ClaI* in order to avoid performing a *FspI* partial digest. The 5.8 and 1.4 kb fragments were isolated and the 1.4 kb fragment was subsequently digested with *FspI*, generating a 1 kb *HindIII/FspI* fragment. To complete the full-length sequence of the 1N/1N chimera, the *FspI/ClaI* PCR product and the vector consisting of the 5.8 kb *ClaI/HindIII* fragment and the 1 kb *HindIII/FspI* fragment were ligated. The chimera was excised from the subclone with *SacII* and *XhoI* and placed into pHa*MDR1*/A (25) generating pHa*MDR1*-1N/1N. The approximately 1.2 kb *NdeI/XhoI*

fragment containing the C-terminal fragment of the *MDR1* gene including the C-terminal ATP site, from pHa*MDR1*-1N/1N was exchanged into pTM1-*MDR1* (wild-type), resulting in pTM1-*MDR1*-1N/1N.

Sequence Analysis. All constructs were sequenced fully in both directions by DNA sequencing on an Applied Biosystems Inc. 377 automated sequencer.

Cell Lines and Viruses. Human HeLa cells were propagated as monolayer cultures at 37 °C in 5% CO₂ in DMEM supplemented with 4.5 g/L glucose, 5 mM L-glutamine, 50 units/mL penicillin, 50 μ g/mL streptomycin, and 10% FBS. Recombinant vaccinia virus encoding bacteriophage T7 RNA polymerase (ν TF7-3), required for the expression of the gene controlled by the T7 promoter in a transfection plasmid or recombinant virus, was obtained from B. Moss (National Institutes of Health, Bethesda, MD). ν TF7-3 was propagated and purified as previously described (26–28). Recombinant vaccinia viruses ν T7*MDR1*(WT) (wild-type P-gp), ν *MDR1*-CM (P-gp-D1200N), ν *MDR1*-Mg5 (P-gp-D555N), and ν *MDR1*-DM (P-gp-D555N/D1200N) were constructed as previously described (28) from the corresponding pTM1-*MDR1* vectors described above.

Trichoplusia ni (High Five; HF) cells (Invitrogen, San Diego, CA) were propagated as monolayer cultures at 27 °C in serum-free ExCell 400 (JRH Biosciences, Lenexa, KS) medium supplemented with an antibiotic–antimycotic (catalog no. 15240-096; Life Technologies, Grand Island, NY) containing 100 units/mL penicillin G, 100 μ g/mL streptomycin sulfate, and 25 μ g/mL amphotericin B (29). Recombinant baculovirus encoding wild-type P-gp containing a six-histidine tag at the C-terminus [BV-*MDR1*(H₆)] was constructed and prepared as described (29).

Expression of Wild-Type P-gp Containing a C-Terminal Six-Histidine Tag in Insect Cells and Preparation of Crude Membranes. Cells grown in T162-cm2 tissue culture flasks (2 \times 10⁷ cells/flask) were infected with BV-*MDR1*(H₆) at a multiplicity of infection of 10 for 2 h in 4 mL of serum-free Ex-Cell 400 medium as described (29). After 2 h, the cells were fed with 16 mL of medium and incubated at 27 °C for 72 h. Crude membranes were prepared as previously described (29).

Expression of P-gp by a Recombinant Vaccinia Virus-Mediated Infection and Infection–Transfection Procedures. A 70–80% confluent monolayer of HeLa cells grown in 75 cm² flasks was infected with ν TF7-3 and transfected with pTM1-*MDR1* as previously described (30). Coinfection of an 80–90% confluent monolayer of HeLa cells grown in a 162 cm² flask with ν TF7-3 and recombinant P-gp-expressing vaccinia viruses was performed as previously described (28).

Antibodies. The human-specific monoclonal antibody MRK-16 was a gift from Hoechst Japan Ltd. (31). The human-specific antibody UIC2 was from Immunotech (Westbrook, ME). Purified mouse IgG2a and FITC-labeled anti-mouse IgG2a secondary antibody were from Pharmingen (San Diego, CA). Goat anti-mouse IgG conjugated with peroxidase was from Life Technologies, Inc. Monoclonal antibody C219 (32) was a gift from Centocor (Malvern, PA). Polyclonal antibody PEPG-2 was developed in this laboratory (33).

Preparation of Crude Membranes. Crude membranes from HeLa cells were made as previously described (5, 30).

SDS–Polyacrylamide Gel Electrophoresis and Immunoblot Analysis. SDS–PAGE and immunoblot analysis were performed as previously described (5, 30). Monoclonal antibody C219 was used at a dilution of 1:1500. The secondary antibody was a 1:10 000 dilution.

Measurement of ATPase Activity. P-gp-associated basal and drug-stimulated ATPase activities of crude membrane preparations were measured as previously described (5, 30) by determining the level of sodium orthovanadate-sensitive release of inorganic phosphate from ATP with a colorimetric method. The vanadate-sensitive activities were calculated as the difference between the ATPase activities obtained in the absence and presence of 300 μ M vanadate.

Fluorescence-Activated Cell Sorting Analysis. FACS analysis was carried out on a FACSort flow cytometer equipped with CellQuest software (Becton Dickinson FACS system, San Jose, CA).

Determination of Cell Surface Expression of P-gp by MRK-16 Staining and FACS Analysis. Cell surface localization of P-gp was determined by use of the monoclonal antibody MRK-16 and FACS analysis as previously described (5, 30), except that the cells were incubated with the antibodies at 37 °C instead of 4 °C.

UIC2 Reactivity Shift Assays. UIC2 shift assays were performed as previously described (5, 30).

Fluorescent Drug Accumulation Assays. Fluorescent drug accumulation assays in intact cells were performed as previously described (5, 30). Calcein-AM, bodipy-FL-forskolin, and bodipy-FL-verapamil were from Molecular Probes (Eugene, OR) and were used at a final concentration of 0.5 μ M. Daunorubicin (Calbiochem, La Jolla, CA) was used at a final concentration of 3 μ M. Measurements of calcein-AM accumulation were taken after a 10 min incubation at 37 °C, whereas for bodipy-FL-forskolin and bodipy-FL-verapamil the cells were incubated for 40 min at 37 °C. The cells were then centrifuged at 200g for 5 min, the medium was removed by aspiration, and the cell pellet was resuspended in 350 μ L of ice-cold PBS and analyzed by FACS. For daunorubicin measurements, the cells were resuspended in 4.5 mL of substrate-free medium with or without cyclosporin A and incubated for an additional 40 min at 37 °C. The cells were pelleted by centrifugation at 200g for 5 min and the medium was removed by aspiration. The cells were then resuspended in 350 μ L of ice-cold PBS and analyzed by FACS.

[α -³²P]-8-Azidoadenosine 5'-Triphosphate Photoaffinity Labeling of P-gp and Immunoprecipitation. Photoaffinity labeling of crude membranes (50–100 μ g) with 2.5 μ M or 80 μ M [α -³²P]-8-azido-ATP followed by immunoprecipitation with PEPG-2 was performed as previously described (5, 30). For ATP hydrolysis/vanadate trapping experiments, membranes were preincubated with 300 μ M vanadate and 25 μ M verapamil for 3 min at room temperature prior to the addition of [α -³²P]-8-azido-ATP. Samples were subsequently incubated at 37 °C for 10 min, followed by the addition of 9 mM unlabeled ATP, photo-cross-linking and immunoprecipitation. Samples were routinely exposed to UV light at 365 nm (Black-Ray lamp, model XX-15; UVP, Upland, CA) for 15 min on ice to facilitate cross-linking.

Drug Photoaffinity Labeling and Immunoprecipitation. Photoaffinity labeling of P-gp with [¹²⁵I]IAAP (specific activity 2200 Ci/mmol) was performed with crude mem-

branes (50–100 μ g) as previously described (30) and followed by immunoprecipitation with polyclonal antibody PEPG-2 (5, 30). Samples were routinely exposed to 365 nm UV light for 15 min on ice to facilitate cross-linking.

Mild Trypsin Digestion of P-gp. As indicated, after photo-cross-linking, the crude membrane preparations from labeling reactions were subjected to mild trypsin digestion. Ten micrograms of trypsin (2 mg/mL in 1 mM HCl) were added to each sample. The reaction was carried out for 5 min at 37 °C. Subsequently, 150 μ g of trypsin inhibitor was added to each reaction, followed by immunoprecipitation. The resultant proteins are referred to as the N-half (~80 kDa) and the C-half (~60 kDa).

Data Analysis. Quantitative phosphorimaging analysis was performed with the STORM System (Molecular Dynamics) and used to calculate the percent inhibition of [α -³²P]-8-azido-ATP labeling of human P-gp (% inhibition) as follows: % inhibition = $\{1 - [([\alpha\text{-}^{32}\text{P}]\text{-8-azido-ATP labeling density in the presence of unlabeled ATP})/([\alpha\text{-}^{32}\text{P}]\text{-8-azido-ATP labeling density in the absence of unlabeled ATP})]\}$ (100). Half-maximum inhibition was estimated from percentage inhibition of [α -³²P]-8-azido-ATP labeling versus unlabeled ATP concentration values by nonlinear least-squares regression (WinNonlin; Statistical Consultants, Inc., Apex, NC) according to the standard Michaelis–Menten equation.

The percentage of apparent maximum [α -³²P]-8-azido-ATP labeling of P-gp in the presence of increasing concentrations of MgCl₂ (% maximum incorporation) was calculated as follows: % maximum incorporation = $\{([\alpha\text{-}^{32}\text{P}]\text{-8-azido-ATP labeling density})/(\text{maximum } [\alpha\text{-}^{32}\text{P}]\text{-8-azido-ATP labeling density})\}$ (100).

RESULTS

Human P-gp Mutants with Amino Acid Substitutions in the Walker B Consensus Sequences Are Expressed at the Cell Surface but Are Devoid of Drug Transport Function and ATPase Activity. To assess the nature of each of the nucleotide binding domains of human P-gp, homologous mutations were made at positions 555 and 1200 in the Walker B consensus motifs of the N- and C-half NBDs (8). These amino acids, which represent the magnesium binding sites (34, 35), were changed from aspartate to asparagine to eliminate the ability to complex and stabilize ATP in the active site. The two mutants, designated P-gp-D555N and P-gp-D1200N, were constructed by site-directed mutagenesis, cloned into pTM1-MDR1, and transiently expressed in HeLa cells coinfecting with the vaccinia virus vTF7-3 as described under Experimental Procedures. As determined by FACS analysis using the human-specific anti-P-gp monoclonal antibody MRK-16 that recognizes an external epitope (31), wild-type P-gp and the two mutant proteins were expressed at the cell surface at high levels compared to vector alone (pTM1) in greater than 80% of the cells (Figure 1A). Total extracts from HeLa cells expressing wild-type P-gp, P-gp-D555N, P-gp-D1200N, and the double mutant P-gp-D555N/D1200N were subjected to immunoblot analysis with the monoclonal antibody C219 (32). While P-gp-D1200N was found to be expressed at a level comparable to wild-type P-gp, in this preparation of membranes it appears that less P-gp-D555N and P-gp D555N/D1200N were expressed

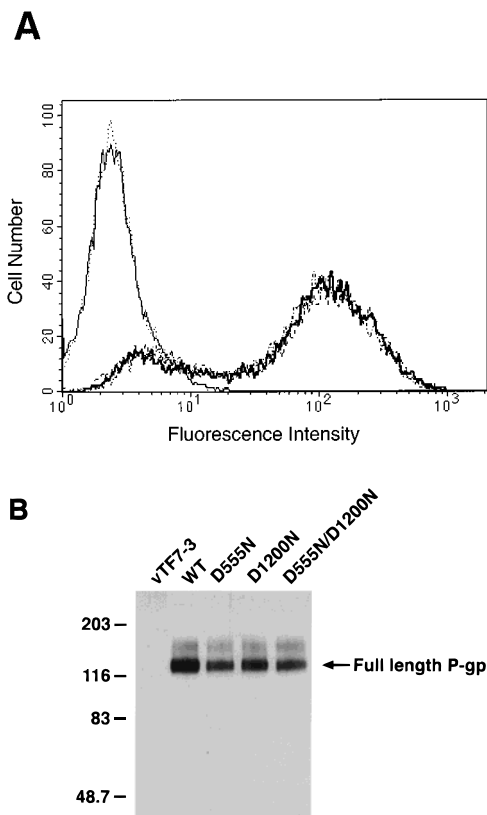


FIGURE 1: Total and cell surface expression of P-gp constructs in HeLa cells using recombinant vaccinia viruses. (A) vTF7-3-infected-transfected HeLa cells (500 000) expressing wild-type P-gp (bold line), P-gp-D555N (---), and P-gp-D1200N (-·-) were subjected to FACS analysis after incubation with 5 μ g of MRK-16 for 30 min at 37 °C, washing (200g, 5 min), and staining with FITC-conjugated anti-mouse IgG secondary antibody (1 μ g) for 30 min at 37 °C. Cells were subsequently washed as described above, resuspended in 400 μ L of cold PBS, and analyzed by FACS. Vector DNA-transfected (pTM1) cells (thin line) and cells incubated with 5 μ g of IgG2a isotype antibody (···) were included as negative controls. (B) Total expression of P-gp by immunoblot analysis. HeLa cells were infected with vTF7-3 recombinant vaccinia viruses expressing wild-type P-gp, P-gp-D555N, P-gp-D1200N, and P-gp-D555N/D1200N and harvested after 48 h. Membranes (1 μ g/lane) prepared from these cells were subjected to SDS-PAGE and immunoblotting with monoclonal antibody C219 (1:1500). Bands were visualized by enhanced chemiluminescence (ECL). The position of P-gp (~140 kDa) is shown by an arrow.

compared to wild-type. A major 140 kDa band was expected since P-gp expressed by the vaccinia virus transient expression system results in an underglycosylated (36), but functional (37–39) form of the molecule. A higher molecular weight band is also apparent that represents more fully glycosylated protein.

Fluorescent substrate accumulation assays were performed on intact HeLa cells expressing wild-type P-gp, P-gp-D555N, and P-gp-D1200N with the P-gp substrate calcein-AM. HeLa cells were transiently infected with vTF7-3 and transfected with pTM1-*MDR1* (wild-type), pTM1-*MDR1*-D555N, and pTM1-*MDR1*-D1200N, with pTM1 as the negative control, and allowed to incubate for approximately 24 h. After incubation with 0.5 μ M calcein-AM for 10 min, cells expressing wild-type P-gp accumulated less substrate than the pTM1 control as measured by a decrease in fluorescence intensity (Figure 2). In the presence of 2 μ M cyclosporin A, P-gp function was inhibited, as demonstrated by increased

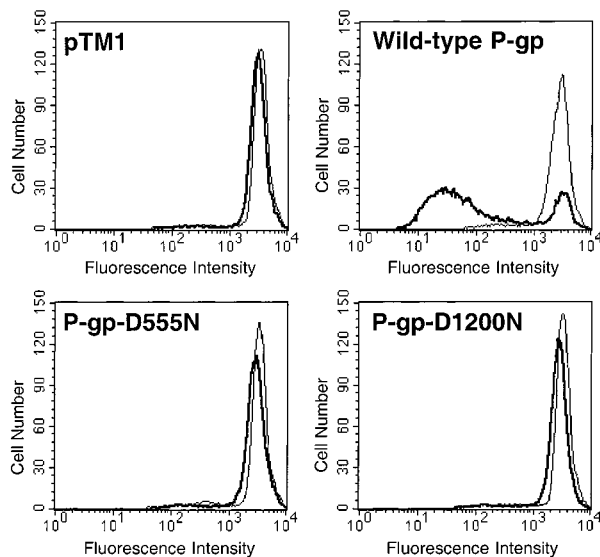


FIGURE 2: Expression and functional analysis of P-gp in transiently infected-transfected HeLa cells. HeLa cells were infected with vTF7-3 and transfected with pTM1-*MDR1* (wild type), pTM1-*MDR1*-D555N, and pTM1-*MDR1*-D1200N for 24 h. Calcein (0.5 μ M) accumulation was determined in these cells by FACS after a 10 min incubation at 37 °C in the presence (thin line) and absence (bold line) of 2 μ M cyclosporin A. vTF7-3-infected cells transfected with pTM1 vector DNA were included as a negative control.

calcein-AM accumulation indistinguishable from that of the pTM1 negative control. Strikingly, the two Walker B mutants P-gp-D555N and P-gp-D1200N were completely devoid of transport function (Figure 2). In both the presence and absence of 2 μ M cyclosporin A, the accumulation patterns for both mutants were similar to those of the pTM1 control and the wild-type protein incubated with cyclosporin A. Similar data were obtained with other fluorescent substrates such as rhodamine 123 and daunorubicin (data not shown). These data suggest that both ATP sites are essential for the transport function of P-gp. Since disruption of either NBD results in a nonfunctional protein, neither the N-half nor the C-half ATP site can function independently of the other.

Basal and Verapamil-Stimulated ATPase Activities of the Walker B Mutant Proteins Are Completely Abrogated, Accounting for the Transport Defects of These Transporters. The ability of Walker B mutants P-gp-D555N, P-gp-D1200N, and P-gp-D555N/D1200N to hydrolyze ATP either in the absence (basal) or presence (drug-stimulated) of 25 μ M verapamil was measured as the vanadate-sensitive release of inorganic phosphate from Mg^{2+} -ATP as described under Experimental Procedures, with membrane preparations from vTF7-3-infected HeLa cells alone or vTF7-3-infected cells that were coinfecting with recombinant vaccinia viruses encoding wild-type P-gp, P-gp-D555N, P-gp-D1200N, and P-gp-D555N/D1200N. Membrane preparations from cells infected with vTF7-3 alone demonstrated an ATPase activity of ~ 5 –7 nmol of P_i released min^{-1} (mg of membrane protein)⁻¹ that did not increase in the presence of verapamil (Figure 3). The basal membrane-associated ATPase activity increased to ~ 12 nmol of P_i released min^{-1} (mg of membrane protein)⁻¹ upon expression of wild-type P-gp. This activity was stimulated approximately 5–6-fold in the presence of 25 μ M verapamil (Figure 3). None of the mutant proteins displayed either basal or verapamil-stimulated ATPase activity above that of the vTF7-3 control (Figure 3). These data

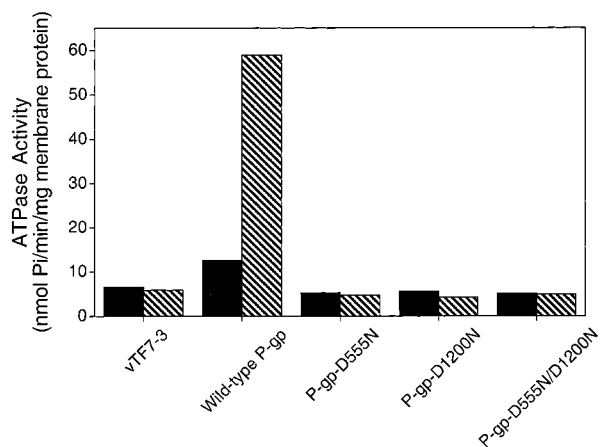


FIGURE 3: Basal and verapamil-stimulated ATPase activities of P-gp in membranes of HeLa cells infected with recombinant P-gp-expressing vaccinia viruses. Membrane preparations from HeLa cells infected with vTF7-3 and coinfecting with vvT7MDR1 (WT) (wild-type P-gp), vvMDR1-CM (P-gp-D1200N), vvMDR1-Mg5 (P-gp-D555N), or vvMDR1-DM (P-gp-D555N/D1200N). The vanadate-sensitive activities shown represent the difference between the ATPase activities measured in the presence and absence of 300 μ M vanadate. Basal activity (solid bars) was measured without the addition of verapamil. Stimulated activity (hatched bars) was determined in the presence of 25 μ M verapamil. Membrane preparations from HeLa cells infected with vTF7-3 alone were used as the negative control.

suggest that the lack of transport function of the mutant proteins (Figure 2) can be attributed to the lack of ATPase activity and that both NBDs need to be functional to generate an active transporter.

[¹²⁵I]IAAP Labeling Is Not Appreciably Affected in the Walker B Mutants of Human P-gp. The drug binding properties of the wild-type and mutant proteins were assessed by photoaffinity labeling with [¹²⁵I]iodoarylazidoprazosin ([¹²⁵I]IAAP), a P-gp substrate. Crude membrane preparations derived from HeLa cells infected with vTF7-3 alone and from cells coinfecting with recombinant vaccinia viruses encoding wild-type P-gp, P-gp-D555N, P-gp-D1200N, and P-gp-D555N/D1200N were labeled with [¹²⁵I]IAAP at a concentration of 7.5 nM, immunoprecipitated with anti-P-gp polyclonal antibody PEPG-2 (33), and subjected to SDS-PAGE and autoradiography (Figure 4A). As expected, no band was observed in the vTF7-3 control lane. Efficient labeling of all of the mutant proteins was observed that was comparable to that of the wild-type protein. These data suggest that mutations made in the Walker B consensus motifs of the N- and C-half NBDs do not affect the ability of the transporter to recognize the substrate [¹²⁵I]IAAP. These data also demonstrate that the antibody PEPG-2 used for immunoprecipitation equally recognizes all of the proteins.

P-gps Containing Mutations in the Walker B Consensus Motif Do Not Demonstrate Vanadate-Induced Inhibition of [¹²⁵I]IAAP Labeling. We have recently shown that ATP hydrolysis is essential for inhibition of [¹²⁵I]IAAP photoaffinity labeling resulting from vanadate-induced nucleotide trapping (29). To further demonstrate that ATP hydrolysis is essential and to evaluate the roles of the two NBDs for inhibition of [¹²⁵I]IAAP labeling as a result of vanadate trapping, we analyzed the effects of the Walker B consensus motif mutations D555N, D1200N, and D555N/D1200N. Crude membrane preparations containing mutant P-gps from

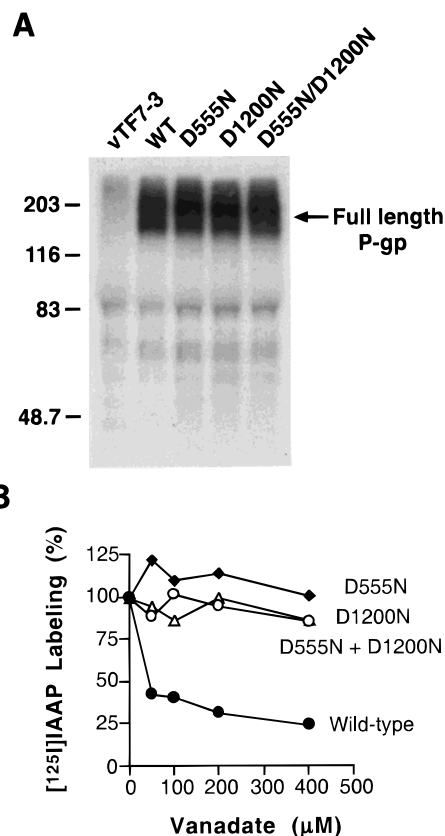


FIGURE 4: [¹²⁵I]IAAP photoaffinity labeling of membranes derived from HeLa cells expressing P-gp and the effect of ATP hydrolysis on labeling. (A) Wild type and the mutant P-gps D555N, D1200N, and D555N/1200N were expressed in HeLa cells by use of recombinant vaccinia viruses, and crude membranes (45 μ g) were used for [¹²⁵I]IAAP photoaffinity labeling. After labeling, P-gp was immunoprecipitated with the polyclonal antibody PEPG-2 and subjected to SDS-PAGE and autoradiography. Full-length P-gp is denoted by an arrow. (B) Effects of mutations in nucleotide binding/utilization sites on vanadate-induced inhibition of [¹²⁵I]IAAP labeling. Wild-type (●) and mutant P-gps, D555N (◆), D1200N (△), and D555N/D1200N (○) were expressed in HeLa cells by use of recombinant vaccinia viruses and crude membranes (15 μ g) were used for [¹²⁵I]IAAP labeling in the presence of varying concentrations of vanadate, 5 mM MgCl₂, and 2.5 mM ATP. After [¹²⁵I]IAAP labeling, samples were analyzed by SDS-PAGE and autoradiography. Radioactivity associated with each band was quantitated and plotted as percent of the zero point control.

HeLa cells infected with recombinant vaccinia viruses were assayed for vanadate-induced inhibition of [¹²⁵I]IAAP labeling. As shown in Figure 4B, inhibition was seen in the wild-type protein, as expected, but in none of the three mutants due to their failure to hydrolyze ATP. These results, taken together with results suggesting that similar mutations made in mouse P-gp are not capable of being vanadate-trapped (40), confirm that ATP hydrolysis and the participation of both nucleotide binding/utilization sites is essential for vanadate-induced inhibition of [¹²⁵I]IAAP labeling. These data also suggest that a conformational change occurs in P-gp upon ATP hydrolysis.

Human P-gp-D555N and P-gp-D1200N Differ Dramatically in Their Ability To Be Labeled with [α -³²P]-8-Azido-ATP. The nucleotide-binding properties of the P-gp constructs were examined by [α -³²P]-8-azido-ATP photoaffinity labeling. Crude membrane preparations were photoaffinity-labeled with [α -³²P]-8-azido-ATP at a concentration of 2.5 μ M at 0

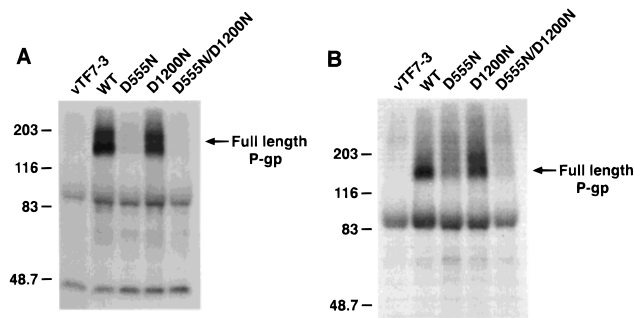


FIGURE 5: [α - 32 P]-8-Azidoadenosine 5'-triphosphate ([α - 32 P]-8-azido-ATP) labeling of P-gp in membrane preparations from HeLa cells. Crude membrane preparations (50 μ g) from HeLa cells infected with vTF7-3 and recombinant vaccinia viruses expressing wild-type P-gp, P-gp-D555N, P-gp-D1200N, or P-gp-D555N/D1200N were photoaffinity-labeled on ice (0 $^{\circ}$ C) with either (A) 2.5 μ M or (B) 77.5 μ M [α - 32 P]-8-azido-ATP. The 77.5 μ M 8-azido-ATP mixture contained 2.5 μ M [α - 32 P]-labeled 8-azido-ATP and 75 μ M unlabeled 8-azido-ATP. Samples were then subjected to immunoprecipitation with polyclonal antibody PEPG-2 as described under Experimental Procedures and eluants were analyzed by SDS-PAGE and autoradiography. Membrane preparations from HeLa cells infected with vTF7-3 alone were used as the negative control. The position of P-gp (~140 kDa) is shown by an arrow.

$^{\circ}$ C in the presence of 10 mM magnesium, immunoprecipitated with PEPG-2, and subjected to SDS-PAGE and autoradiography (Figure 5A). An equivalent amount of crude membranes derived from vTF7-3-infected cells alone was used as a control, and as expected, no band was observed. Membranes expressing wild-type P-gp and P-gp-D1200N were labeled with [α - 32 P]-8-azido-ATP. This labeling was strictly dependent upon magnesium, as incubation in magnesium-free buffer in the presence of 500 μ M EDTA completely eliminated labeling (data not shown). Strikingly, the [α - 32 P]-8-azido-ATP labeling observed in membranes expressing P-gp-D555N and P-gp-D555N/D1200N was severely impaired. This observed phenotype was not due to differential recognition of the mutants by PEPG-2, as all constructs were equally recognized as demonstrated above for [125 I]IAAP labeling (Figure 4A). These results suggest that the ability to bind ATP to the N-half ATP site, as determined by photoaffinity labeling, is eliminated or reduced significantly in the protein containing a mutation in the magnesium binding site (D555N). Binding to the C-half ATP site is apparently severely compromised in this mutant, although the site is intact. This decreased labeling may be a result of the mutation itself or to an inherent reduced ability of the C-half site to be photolabeled with 8-azido-ATP, even in the wild-type molecule. The same experiment was subsequently performed at a saturating concentration of 77.5 μ M [α - 32 P]-8-azido-ATP, and under these conditions, the same differential labeling phenomenon is observed, although slightly more label is incorporated into P-gp-D555N (Figure 5B).

N-Half of Human P-gp Is Preferentially Labeled with [α - 32 P]-8-Azido-ATP at 0 $^{\circ}$ C. To further elucidate the nature of the [α - 32 P]-8-azido-ATP photoaffinity labeling of human P-gp, crude membranes were first photoaffinity-labeled and then subjected to mild trypsin digestion in order to separate the two halves of the protein. Immunoprecipitation, SDS-PAGE, and autoradiography followed these steps. P-gp has one trypsin-sensitive site located within the linker region between amino acids 653 and 686 (41). Digestion at this

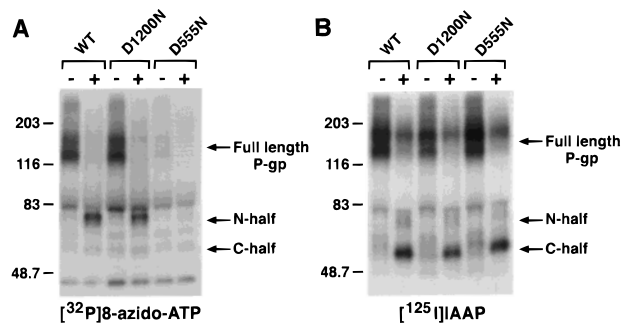


FIGURE 6: [α - 32 P]-8-Azido-ATP and [125 I]IAAP photoaffinity labeling and trypsinization of membranes prepared from HeLa cells expressing P-gp. Crude membrane preparations (50–60 μ g) from HeLa cells infected with vTF7-3 and recombinant vaccinia viruses expressing wild-type P-gp, P-gp-D555N, P-gp-D1200N, or P-gp-D555N/D1200N were photoaffinity-labeled with either (A) [α - 32 P]-8-azido-ATP (2.5 μ M) or (B) [125 I]IAAP (15 nM) as described in the legend to Figures 4 and 5. After UV cross-linking, samples indicated by the (+) were subjected to mild trypsin digestion as described under Experimental Procedures prior to immunoprecipitation with PEPG-2, SDS-PAGE, and autoradiography. The position of full-length P-gp (~140 kDa), the 80 kDa N-terminal half (N-half), and the 60 kDa C-terminal half (C-half) are shown by the arrows. The identities of the fragments were further confirmed by immunoblot analysis.

site results in the generation of two large fragments, an 80 kDa N-half and a 60 kDa C-half, both of which can be recognized by the polyclonal antibody PEPG-2 (33) in immunoprecipitation reactions. As can be seen, the N-half of P-gp is labeled predominantly in the wild-type and D1200N proteins (Figure 6A). As was demonstrated in Figure 5, again, no substantial labeling was observed for P-gp-D555N. Under the conditions of these assays, these data are consistent with a model in which ATP binding is asymmetric, resulting predominantly in labeling of the N-half. Labeling of the C-half under ATP binding conditions (0 $^{\circ}$ C) is limited, perhaps because the site is obscured or inaccessible to the [α - 32 P]-8-azido-ATP molecule.

To confirm that the C-half was, in fact, immunoprecipitated in the reaction, [125 I]IAAP photoaffinity labeling was performed in parallel under conditions where the C-half was preferentially labeled using a concentration of 15 nM (42). These reaction mixtures were photoaffinity-labeled, digested with trypsin, immunoprecipitated with PEPG-2, and subjected to SDS-PAGE and autoradiography (Figure 6B). As shown in Figure 6B, all of the full-length P-gp constructs were labeled comparably, and upon trypsin digestion, labeling of the C-half of each of the proteins was roughly equivalent. These data confirm that the C-half is immunoprecipitable and that the differences seen between the constructs in [α - 32 P]-8-azido-ATP labeling experiments were not artifacts of the procedure. The identities of the N- and C-halves of P-gp were further confirmed by immunoblot analysis with antibodies specific to these fragments (data not shown). Additionally, quantitation of the full-length protein and both halves confirmed that 85–95% of the [α - 32 P]-8-azido-ATP label was recovered after trypsinization and immunoprecipitation (data not shown). This analysis also confirmed that 75% of the 32 P label was localized to the N-half of the protein and 25% was localized to the C-half.

C-Half of Human P-gp Is Preferentially Labeled with [α - 32 P]-8-Azido-ATP at 37 $^{\circ}$ C in the Presence of Vanadate. We next used orthovanadate (vanadate; V_i) trapping to

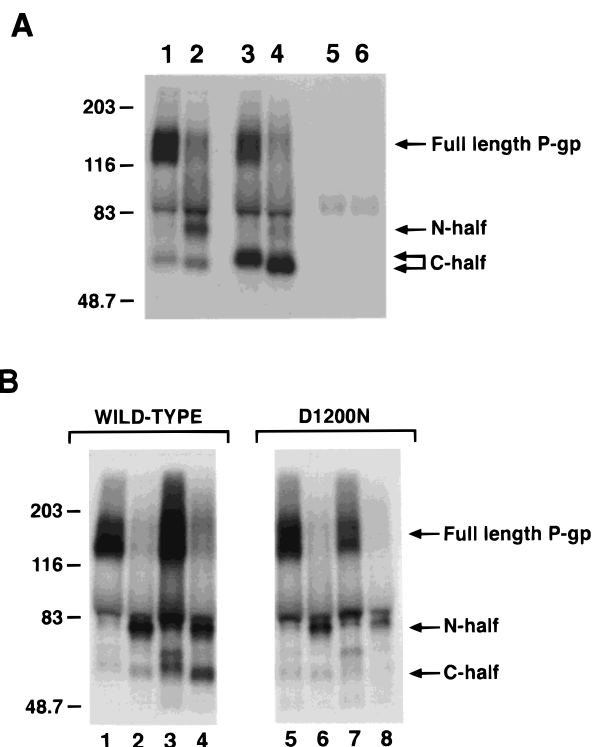


FIGURE 7: [α - 32 P]-8-Azido-ATP photoaffinity labeling and vanadate trapping of wild-type and P-gp-D1200N from HeLa cell membranes. Crude membrane preparations (100 μ g) from HeLa cells infected with vTF7-3 and the recombinant vaccinia virus expressing wild-type or P-gp-D1200N were photoaffinity-labeled with 2.5 μ M [α - 32 P]-8-azido-ATP for 10 min. As indicated below, 9 mM cold ATP was added to the sample after incubation at the appropriate temperature and allowed to incubate for an additional 3 min. No excess unlabeled ATP was added to the samples shown in panel B. Trypsinization was performed as described under Experimental Procedures after 15 min of UV cross-linking on ice. (A) Separation of ATP binding and hydrolysis labeling properties of wild-type P-gp. Lane 1, 0 $^{\circ}$ C, (-) trypsin; lane 2, 0 $^{\circ}$ C, (+) trypsin; lane 3, 37 $^{\circ}$ C, (+) 300 μ M vanadate, (+) 25 μ M verapamil, (+) 9 mM unlabeled ATP, (-) trypsin; lane 4, 37 $^{\circ}$ C, (+) 300 μ M vanadate, (+) 25 μ M verapamil, (+) 9 mM unlabeled ATP, (+) trypsin; lane 5, 0 $^{\circ}$ C, (+) 9 mM unlabeled ATP, (-) trypsin; lane 6, 0 $^{\circ}$ C, (+) 9 mM unlabeled ATP, (+) trypsin. (B) Examination of wild-type P-gp (lanes 1–4) and D1200N P-gp (lanes 5–8) under [α - 32 P]-8-azido-ATP hydrolysis/binding conditions: lanes 1 and 5, 0 $^{\circ}$ C, (-) trypsin, (-) 300 μ M vanadate; lanes 2 and 6, 0 $^{\circ}$ C, (+) trypsin, (-) 300 μ M vanadate; lanes 3 and 7, 37 $^{\circ}$ C, (+) 300 μ M vanadate, (+) 25 μ M verapamil; lanes 4 and 8, 37 $^{\circ}$ C, (+) 300 μ M vanadate, (+) 25 μ M verapamil, (+) trypsin. For all samples, after UV cross-linking and trypsinization (as indicated), the reactions were immunoprecipitated with PEPG-2 and subjected to SDS-PAGE and autoradiography. The positions of full-length P-gp (\sim 140 kDa), the 80 kDa N-terminal half (N-half), and the 60 kDa C-terminal half (C-half) are shown by the arrows. The identities of the fragments were further confirmed by immunoblot analysis.

elucidate the labeling pattern under conditions where ATP was hydrolyzed. This technique allows for the visualization of one cycle of ATP hydrolysis (43). Since the affinity of the $Mg \cdot ADP \cdot V_i$ complex is very high, the addition of a large excess of unlabeled ATP ensures visualization of the postreaction complex under hydrolysis conditions in the presence of vandate. As shown in Figure 7A, samples in lanes 1, 3, and 5 represent the intact molecule and those in 2, 4, and 6 represent trypsin-treated membranes. Lanes 1 and 2 were reactions incubated under binding conditions (0 $^{\circ}$ C) and show the predominant N-half distribution of label

(75% N-half and 25% C-half) as observed previously in Figure 6A. Lanes 5 and 6 (Figure 7A) were reactions incubated under binding conditions (0 $^{\circ}$ C), but a large excess of unlabeled ATP was added before photo-cross-linking. Furthermore, no labeling of P-gp was observed at 0 $^{\circ}$ C in the presence of vanadate after addition of a 9 mM excess of cold ATP to the reaction mixture, suggesting that no hydrolysis occurred under binding conditions (data not shown). Lanes 3 and 4 represent reactions incubated in the presence of vanadate and 25 μ M verapamil at 37 $^{\circ}$ C with an added 9 mM excess of unlabeled ATP after the incubation and before photo-cross-linking. These data show that, upon hydrolysis, the C-half of P-gp is preferentially labeled in the postreaction complex with [α - 32 P]-8-azido-ADP (Figure 7A, lane 4). In parallel reactions in which no excess unlabeled ATP was added following hydrolysis and prior to photo-cross-linking, labeling of the N-half was also observed in the wild-type protein (Figure 7B, lane 4). The labeling of the N-half was similar to that observed under binding conditions alone (Figure 7B, lane 2), suggesting that [α - 32 P]-8-azido-ATP can be bound to the N-half ATP site when hydrolysis has occurred at the C-half site. There was no apparent increase in the amount of label associated with the C-half of P-gp-D1200N under hydrolysis conditions, suggesting that the mutant is incapable of catalyzing even one ATP hydrolysis reaction (Figure 7B, lane 8). However, the N-half of P-gp-D1200N retained its ability to be labeled with [α - 32 P]-8-azido-ATP (Figure 7B, lanes 6 and 8) under both binding and hydrolysis conditions. Similar to P-gp-D1200N, P-gp-D555N and P-gp-D555N/D1200N were not capable of being vanadate-trapped, confirming their lack of ATPase activity (data not shown).

Upon incubation with vanadate and UV light, a side reaction occurs, resulting in peptide bond cleavage at or in close proximity to the lysine/arginine-rich trypsin-sensitive region within the linker region (20, 44), accounting for the presence of a slightly larger C-terminal fragment in the non-trypsin-treated sample (Figure 7A, lane 3, top arrow of C-half). Exogenously added [α - 32 P]-8-azido-ADP, made by hydrolysis of [α - 32 P]-8-azido-ATP with an ATP phosphatase from dog kidney, produces a labeling pattern that mimics that of [α - 32 P]-8-azido-ATP, with the label predominantly in the N-half of P-gp (data not shown), suggesting that in situ hydrolysis of ATP must occur to label the C-half of the protein. Taken together, these data suggest that a conformational change occurs upon ATP hydrolysis, making the C-half accessible for labeling. Furthermore, the data suggest that under these assay conditions, binding to the N-half site allows or is necessary for hydrolysis at the C-half site and that this transition species may not hydrolyze ATP at the N-half site.

Wild-Type and D1200N Human P-gp Proteins Do Not Differ Significantly in Their Apparent Affinity for ATP. To determine the amounts of ATP necessary for 50% inhibition of [α - 32 P]-8-azido-ATP photoaffinity labeling, a rough indicator of the apparent affinities of the various P-gp constructs for ATP, membranes from HeLa cells expressing the P-gp constructs were photoaffinity-labeled with [α - 32 P]-8-azido-ATP in the presence of increasing concentrations (0–5 mM) of unlabeled ATP, immunoprecipitated with PEPG-2, and subjected to SDS-PAGE and autoradiography. The specific P-gp bands were quantified by phosphorimaging and the data were analyzed as described under Experimental

Table 1: Inhibition of [α - 32 P]-8-Azido-ATP Photoaffinity Labeling of Human P-Glycoprotein by ATP

P-glycoprotein construct	concn of ATP (μ M) Required for 50% Inhibition of [α - 32 P]-8-azido-ATP ^a Labeling ^b
wild-type P-gp ^c	12.8 \pm 0.2
P-gp-D1200N ^c	9.7 \pm 0.1

^a Protein was labeled with approximately 2.5 μ M [α - 32 P]-8-azido-ATP. Data were analyzed as described under Experimental Procedures. ^b Data represent mean \pm standard error. ^c P-gp was derived from HeLa cells infected with recombinant vaccinia viruses.

Procedures. By this assay, P-gp proteins were inhibited by ATP in a concentration-dependent manner with half-maximal inhibition of 12.8 \pm 0.2 μ M for wild-type P-gp and 9.7 \pm 0.1 for P-gp-1200N (Table 1). Under the conditions of this assay, P-gp-D555N was labeled poorly, precluding the reliable estimation of the concentration required for 50% inhibition of labeling by ATP for this construct. These data suggest that the wild-type and P-gp D1200N mutant proteins have similar apparent affinities for ATP. Under the conditions of the assay, the binding capacity of the C-site, as demonstrated by labeling of P-gp-D555N, is limited and could not be reliably quantitated. Under these conditions, no apparent cooperativity was observed in the [α - 32 P]-8-azido-ATP photoaffinity labeling of any of the P-gp constructs examined.

Inactive Walker B P-gp Mutants Exist in a Transport-Incompetent Conformation at the Cell Surface, Based on Interaction with the Conformation-Sensitive Monoclonal Antibody UIC2. To determine if conformational differences exist between active wild-type Pgp and inactive P-gp-D555N and P-gp-D1200N, the reactivity of these constructs expressed transiently in HeLa cells was assessed by use of the conformation-sensitive monoclonal anti-human P-gp antibody UIC2 (5, 45). As shown in Figure 8, the population of cells expressing the wild-type P-gp protein demonstrates a significant shift in fluorescence intensity upon the addition of 5 μ M cyclosporin A, a P-gp substrate. In contrast, this shift is not observed with either of the Walker B mutant proteins in either the presence or absence of cyclosporin A, as demonstrated by the superimposability of the two populations (Figure 8). Furthermore, the UIC2 reactivity of cells expressing either P-gp-D555N and P-gp-D1200N is indistinguishable from each other, in either the presence or absence of cyclosporin A, and is equivalent to that of the cyclosporin A-treated wild-type-expressing cells. These UIC2 reactivity data, taken together with the ATPase data that demonstrated complete abrogation of ATPase activity for the D555N and D1200N P-gp proteins (Figure 3) and the ATP labeling data that demonstrated marked differences in the ability of these molecules to bind ATP (Figure 5), strongly suggest that the intrinsic ability of the P-gp molecule to hydrolyze ATP or associate with hydrolysis products accounts for the difference in conformation detected by UIC2.

Concentration of Magnesium Required for Half-Maximal [α - 32 P]-8-Azido-ATP Labeling of Wild-Type P-gp Is Approximately 50 Times Higher Than the [α - 32 P]-8-Azido-ATP Concentration. Since the mutations made in the Walker B motif were designed to affect magnesium binding or coordination, the influence of Mg²⁺ concentration on [α - 32 P]-8-azido-ATP labeling was examined. Crude membrane preparations from HeLa cells expressing either wild-type

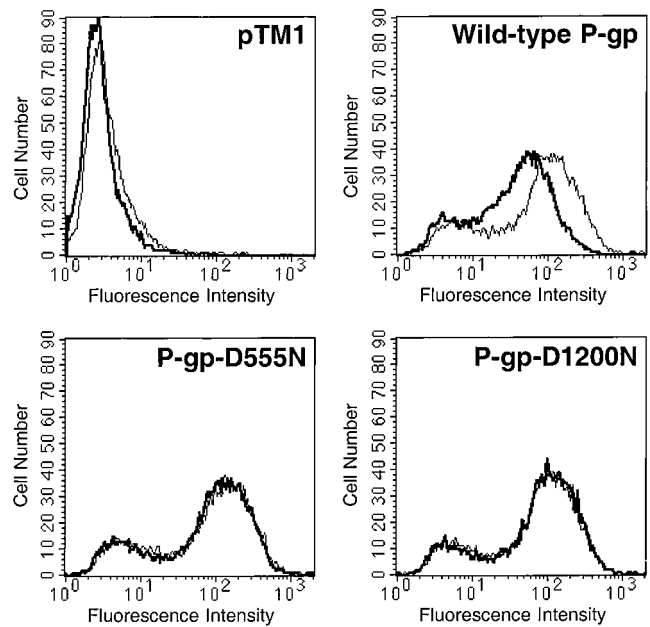


FIGURE 8: UIC2 reactivity shift induced by incubation with cyclosporin A. vTF7-3-infected-transfected HeLa cells expressing wild-type P-gp, P-gp-D555N, or P-gp-D1200N were subjected to FACS analysis after staining with UIC2 in the presence (thin line) and absence (bold line) of 5 μ M cyclosporin A. Vector DNA-transfected (pTM1) cells were included as a negative control. A total of 500 000 cells were preincubated for 3 min at 37 $^{\circ}$ C and for an additional 5 min with or without 5 μ M cyclosporin A (final concentration) in a final volume of 400 μ L. Subsequently, 5 μ g of UIC2 was added to the cell suspensions and allowed to incubate at 37 $^{\circ}$ C for 30 min. The cell suspensions were then diluted to 5 mL in IMDM supplemented with 5% FBS and centrifuged at 200g for 5 min. Washed cell pellets were resuspended in 400 μ L of medium containing 1 μ g of FITC-labeled anti-mouse IgG and incubated at 37 $^{\circ}$ C for 30 min. Cells were washed as above, resuspended in 400 μ L of cold PBS, and analyzed by FACS.

P-gp or P-gp-D1200N were incubated and photoaffinity-labeled in the presence of increasing MgCl₂ (0–10 mM) followed by immunoprecipitation with PEPG-2, SDS-PAGE, and autoradiography. The signal was quantified by phosphorimaging analysis and the percent maximum incorporation was calculated as described under Experimental Procedures. Figure 9 demonstrates that for both the wild-type P-gp (Figure 9A) and P-gp-D1200N (Figure 9B) the labeling with [α - 32 P]-8-azido-ATP increased in a magnesium concentration-dependent manner with half-maximum incorporation at 152.9 \pm 29.9 μ M for wild-type P-gp and 161.5 \pm 39.7 μ M for P-gp-D1200N. The extremely low labeling efficiency of P-gp-D555N precluded analysis of that protein in this assay. For comparison, the same assay was performed on wild-type P-gp-H₆ derived from membranes from baculovirus-infected insect cells (Figure 9A, inset) in which a comparable value of 86.7 \pm 14.2 μ M was obtained. No apparent cooperativity was observed with increasing concentrations of MgCl₂ in the [α - 32 P]-8-azido-ATP photoaffinity labeling studies of any of the P-gp constructs examined. Taken together, these data demonstrate that the P-gp-D1200N and wild-type P-gp proteins have similar requirements for Mg²⁺ and that the requirement is 50–60 times greater than the [α - 32 P]-8-azido-ATP concentration (2.5 μ M) used in the assay, suggesting another role for magnesium in addition to complexing with ATP in the active site.

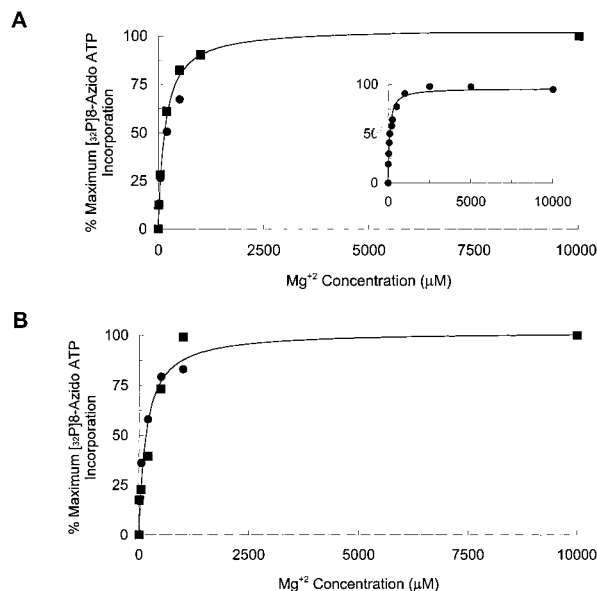


FIGURE 9: Effect of increasing concentrations of MgCl_2 on $[\alpha\text{-}^{32}\text{P}]$ -8-azido-ATP photoaffinity labeling of wild-type P-gp and P-gp-D1200N in membrane preparations from HeLa cells. Crude membrane preparations ($75 \mu\text{g}$) from HeLa cells expressing (A) wild-type P-gp and (B) P-gp-D1200N were photoaffinity-labeled with $2.5 \mu\text{M}$ $[\alpha\text{-}^{32}\text{P}]$ -8-azido-ATP on ice (0°C) in the presence of increasing concentrations of MgCl_2 (0 – 10 mM). The zero point sample was labeled in magnesium-free buffer containing $500 \mu\text{M}$ EDTA. After photo-cross-linking, the samples were immunoprecipitated with PEPG-2 anti-P-gp polyclonal antibody and subjected to SDS-PAGE and autoradiography. Membranes ($35 \mu\text{g}$) from baculovirus-infected insect cells expressing wild-type P-gp-H₆ were examined similarly (inset, panel A) but without subsequent immunoprecipitation. The signals were quantitated by phosphorimaging analysis (Storm System; Molecular Dynamics). The line represents the fit of the Michaelis–Menten model to the data by nonlinear least-squares regression analysis. The filled squares and circles represent two different experiments.

Chimeric Human P-gp Molecule That Contains Two N-Terminal ATP-Binding Domains Is Expressed at the Cell Surface and Is Functional for Transport. To study the basis for the asymmetry of the two ATP sites, a chimeric P-gp molecule containing two N-terminal nucleotide binding domains was constructed and expressed in HeLa cells by the vaccinia virus expression system. The resultant protein, P-gp-1N/1N, is composed of wild-type P-gp sequence from amino acid positions 1 through 1062, continues with amino acids 420–562, and then resumes with amino acid 1208 and continues to 1280. Wild-type P-gp and P-gp-1N/1N were expressed transiently with vTF7-3 in HeLa cells and analyzed for cell surface expression and function by FACS analysis after 24 h (Figure 10). As shown in panel A, both wild-type P-gp and P-gp-1N/1N were expressed at comparable levels at the cell surface as determined by MRK-16 antibody staining. These cells were then analyzed for function using fluorescent drug accumulation assays with the P-gp substrates bodipy-FL-forskolin ($0.5 \mu\text{M}$) (panel B), bodipy-FL-verapamil ($0.5 \mu\text{M}$) (panel C), and daunorubicin ($3 \mu\text{M}$) (panel D). After incubation with bodipy-FL-forskolin (panel B), cells expressing both constructs accumulated less substrate than the cells treated with $5 \mu\text{M}$ cyclosporin A, a potent inhibitor of P-gp function (5, 23, 46). These data demonstrate that P-gp-1N/1N is as functional as wild-type P-gp for exclusion of this substrate from the P-gp-expressing cells and that this transport function is inhibitable by a known

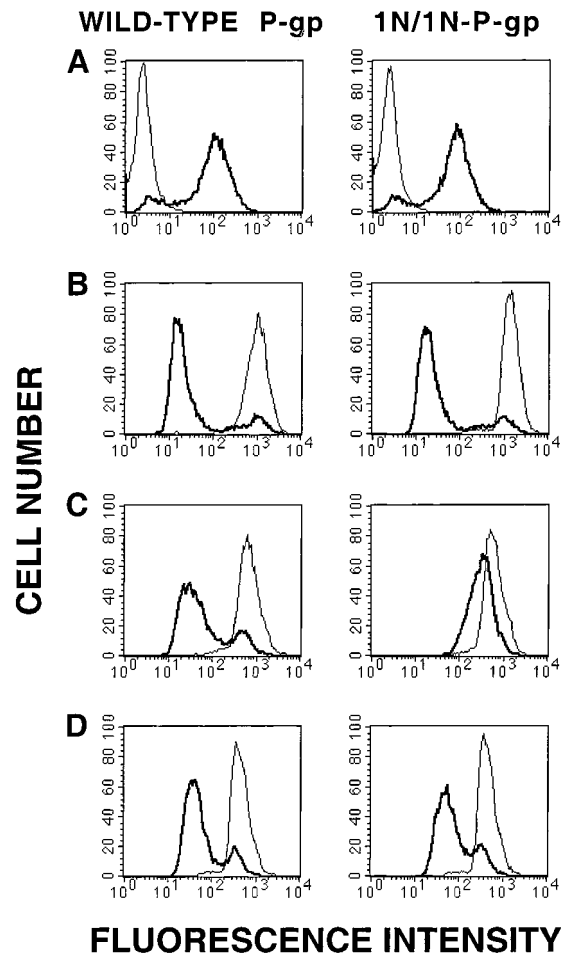


FIGURE 10: Expression and functional analysis of P-gp in transiently infected–transfected HeLa cells expressing wild-type P-gp and the nucleotide binding domain chimera P-gp-1N/1N. HeLa cells were infected with vTF7-3 and transfected with pTM1-MDR1 (wild type) (left side panels) and pTM1-MDR1-1N/1N (right side panels) for 24 h. (A) Cells were subjected to FACS analysis after MRK-16 staining (bold line). Samples were assayed in parallel with the IgG2a isotype control antibody (thin line). (B) Bodipy-FL-forskolin ($0.5 \mu\text{M}$), (C) bodipy-FL-verapamil ($0.5 \mu\text{M}$), and (D) daunorubicin ($3 \mu\text{M}$) accumulation was determined in these cells in the presence (thin line) and absence (bold line) of $5 \mu\text{M}$ cyclosporin A.

P-gp reversing agent. However, it appears that P-gp-1N/1N is less efficient than wild-type in excluding bodipy-FL-verapamil and, to a lesser extent, daunorubicin (panels C and D). In constructing this protein, three amino acid changes were introduced: K1061R, V1214I, and Q1215D. These changes, which are in amino acids that are located outside of the NBD, when introduced into wild-type P-gp do not appear to have any effects on the ability of P-gp to confer drug resistance (data not shown). These data suggest that the two nucleotide binding domains are partially interchangeable.

N-Terminal Half of the 1N/1N-P-gp Chimera Is Also Preferentially Labeled with $[\alpha\text{-}^{32}\text{P}]$ -8-Azido-ATP at 0°C . To determine the nature of the nucleotide binding domains in the P-gp-1N/1N molecule, $[\alpha\text{-}^{32}\text{P}]$ -8-azido-ATP photoaffinity labeling at 4°C was performed with wild-type P-gp and P-gp-1N/1N, followed by mild trypsin digestion, to separate the two halves of the proteins, and immunoprecipitation with PEPG-2. As shown in Figure 11, both the wild-type (WT) P-gp and the P-gp-1N/1N molecules were labeled

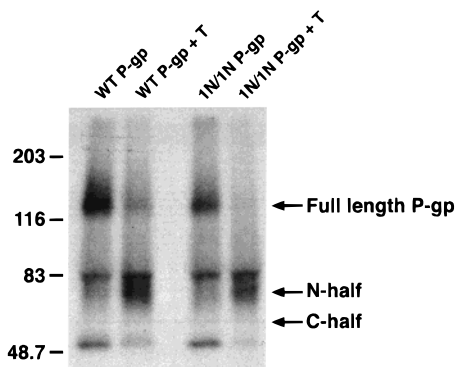


FIGURE 11: [α - 32 P]-8-azido-ATP photoaffinity labeling and trypsinization of membranes prepared from HeLa cells expressing wild-type P-gp and the P-gp-1N/1N nucleotide binding domain chimera. Crude membrane preparations (100 μ g) from HeLa cells infected with vTF7-3 and transfected with pTM1-*MDR1* (wild type) and pTM1-*MDR1*-1N/1N for 48 h were photoaffinity-labeled with [α - 32 P]-8-azido-ATP as described in the legend to Figure 5. After UV cross-linking for 15 min on ice, samples indicated by the + T were subjected to mild trypsin digestion as described under Experimental Procedures prior to immunoprecipitation with PEPG-2, SDS-PAGE, and autoradiography. The positions of full-length P-gp (~140 kDa), the 80 kDa N-terminal half (N-half), and the 60 kDa C-terminal half (C-half) are shown by the arrows.

with [α - 32 P]-8-azido-ATP. When the P-gp proteins were cut with trypsin, the label was predominantly localized to the N-half of the protein for both wild-type P-gp and P-gp-1N/1N. In control experiments, [125 I]IAAP labeling was seen in the C-half, proving that it was intact and present (data not shown). These data suggest that the asymmetry of the two ATP sites does not result from the difference in primary sequence of the N-half NBD and the C-half NBD but resides in their location in P-gp.

DISCUSSION

Human P-glycoprotein is an ATP-dependent membrane transporter that is responsible, in part, for the phenotype of multidrug resistance in a variety of cancers. It is composed of two homologous halves, each containing two similar but not identical ATP binding/utilization domains (2). Through the studies presented here, we have demonstrated that both of the ATP sites are essential but behave asymmetrically in intact P-gp. The two sites were shown to be essential since mutations in each of the Walker B consensus motifs inactivate function. These mutations at positions D555N and D1200N, made separately or in concert, did not affect the ability of the transporter to bind substrate but completely abrogated transport function and both basal and drug-stimulated ATPase activity. P-gp containing these mutations also did not demonstrate vanadate-induced inhibition of [125 I]-IAAP labeling, an indicator of the ability of the transporter both to catalyze hydrolysis of one ATP molecule and to undergo a hydrolysis-dependent conformational change (29). Analysis of conformational differences between the inactive and wild-type P-gp molecules using the monoclonal antibody UIC2 (45) also revealed conformational differences between the proteins and suggested that the wild-type protein may pass through a non-hydrolysis-competent state during the normal drug transport process.

The magnesium dependence of P-gp-associated ATPase activity and [α - 32 P]-8-azido-ATP labeling has been previ-

ously demonstrated (5, 47–49), but its concentration dependence has not been fully explored. We determined that a vast excess of magnesium (150 μ M) in relation to [α - 32 P]-8-azido-ATP (2.5 μ M) was required for half-maximal labeling of P-gp. This value is approximately 50–60 times the concentration necessary for generation of the Mg \cdot ATP complex, generally considered to be at least in a 1:1 or 2:1 ratio with the ATP concentration. Recently, similar observations have also been made in our laboratory with a soluble protein encoding the N-half nucleotide binding domain (C. L. Booth, L. Pulaski, M. M. Gottesman, and I. Pastan, unpublished data). These data suggest that magnesium may be playing an additional role in stabilizing or ordering the active site of P-gp or in exerting a structural change in the entire protein.

We demonstrated the asymmetry of the two ATP sites through the study of [α - 32 P]-8-azido-ATP labeling properties of the wild-type transporter using subsaturating concentrations. Our data indicate that the sites are differentially photolabeled in conformations in which ATP is hydrolyzed and in conformations in which ATP cannot be hydrolyzed, since we observed predominant labeling of the N-half of wild-type P-gp under binding conditions and predominant labeling of the C-half of wild-type P-gp at 37 $^{\circ}$ C in the presence of vanadate.

Additional evidence as to the asymmetry of the two sites came out of studies with the P-gp constructs containing mutations in the Walker B motifs of each NBD. Whereas P-gp-D1200N, the mutant transporter with a C-terminal amino acid substitution, labels comparably to the wild-type protein, P-gp-D555N, containing a homologous N-terminal mutation, is severely impaired in its ability to be labeled with [α - 32 P]-8-azido-ATP. The inability of P-gp-D555N to be labeled efficiently even though the C-half NBD was intact may be because the mutation severely affected the ability of Mg \cdot ATP to bind to the N-half NBD, and the protein exists in such a conformation that either the C-half NBD site is obscured from nucleotide or the amino acid to which the azido group is to be cross-linked is improperly positioned. This hypothesis that the N-half NBD was impaired for labeling in the D555N protein was supported through analysis of the labeling pattern of the two halves of the molecule. After mild trypsinization, it was apparent that the N-half is predominantly labeled in the D1200N and wild-type proteins, whereas little to no labeling of the N-half of the P-gp-D555N was observed. Taken together, these data suggest that the two potential ATP sites are not identical and are asymmetrically arranged in the intact P-gp molecule.

We also constructed a chimeric P-gp molecule that contains two identical N-half ATP binding cassettes and explored its drug transport and [α - 32 P]-8-azido-ATP labeling properties. This molecule was expressed equivalently at the cell surface compared to wild-type P-gp and retained the ability to transport fluorescent substrates, though not to the same degree for all substrates tested. The nucleotide binding properties of this molecule reflected those of wild-type P-gp; i.e., it bound [α - 32 P]-8-azido-ATP comparably and the label was predominantly localized to the N-half of the protein. Since the primary sequence of the two NBDs is identical, this differential labeling may reflect an asymmetric arrangement of the two NBDs in the intact molecule. Several other P-gp chimeras were also constructed, including molecules

containing two identical C-terminal nucleotide binding domains and one in which the two sites were interchanged in the same molecule (P. Wu., U. A. Germann, C. A. Hrycyna, I. Pastan, and M. M. Gottesman, unpublished data). These chimeras, named P-gp-1C/1C and P-gp 1C/1N, were defective in cell surface expression. The 1C/1C protein retained some transport ability, commensurate with its cell surface localization, whereas the 1C/1N protein, though expressed somewhat at the cell surface, was completely devoid of activity. These data suggest that the two NBDs are only partially interchangeable, presumably due to folding defects.

From the work presented here taken together with previous data, it is clear that significant cross-talk exists between the two ATP sites. Mutations made in the Walker A and B consensus motifs abrogate drug transport function and ATPase activity (14–16, 40). Upon removal of amino acids 653–686 from the linker region of human P-gp, the ability of the transporter to confer drug resistance was eliminated along with the ability to transport fluorescent substrates and basal and drug-stimulated ATPase activity (5). These data are of particular interest given that both ATP sites are otherwise intact, suggesting that the interaction or communication between the sites was disrupted in this construct. Furthermore, it has been shown that vanadate trapping of nucleotide at one site prevented ATP hydrolysis at the other site (43) and that chemical modifications that disrupted one site prevented catalysis at the other site (19, 50, 51, 52). Recently, we have provided direct evidence demonstrating that both sites are catalytically active but do not hydrolyze ATP simultaneously (20). These data are consistent with a model for the catalytic cycle of ATPase activity, originally proposed by Senior and colleagues, which postulates that there are two ATP sites that are distinct but in close communication and alternate catalytically (18, 53).

In our current studies, we sought to begin to address the question of just how the two ATP sites communicate. Using a subsaturating concentration of 8-azido-ATP, we have dissected the catalytic cycle and visualized one ordered hydrolytic event in which we propose that binding of ATP to the N-half represents the signal for ATP hydrolysis at the C-half. We have demonstrated that, under hydrolysis conditions, the C-half is labeled by hydrolyzed ATP and the N-half can be photolabeled with 8-azido-ATP. These data further suggest that the ATP site which results in labeling of the C-half is more efficient at hydrolyzing ATP or that the release of ADP from that site is significantly slower than at the other site.

This model is also consistent with the data from the nonfunctional Walker B motif mutants, P-gp-D555N and P-gp-D1200N. The inability of the molecules to function can be connected to their nucleotide photoaffinity labeling characteristics. In the case of P-gp-D555N, only the C-half is intact. The N-half is not able to bind ATP, thereby preventing the hydrolysis signal from being transmitted to the C-half. In the case of P-gp-D1200N, although the N-half can bind ATP, the C-half is disabled by the mutation and the molecule remains hydrolysis-incompetent. These data are consistent with a model in which the binding of nucleotide at the second site is indispensable for hydrolysis at the other site, originally proposed by Senior and colleagues (18, 53).

The present models for the catalytic cycle of P-gp suggest that each hydrolysis event is coupled to transport of a drug

molecule (18, 29), although thus far it has only been possible to visualize half of the cycle. The hydrolysis of ATP has been shown to be linked to a conformational change in the protein that moves the drug molecule from the initial interaction site to a site where it can be released from the molecule along with phosphate (29; this work), resulting in a molecule that has an altered affinity for substrate. In this model, release of ADP has been proposed to regenerate the high-affinity drug-binding molecule, readying it for binding by another ATP and subsequent hydrolysis. This second part of the catalytic cycle could thus be used for transport of another drug molecule.

Through the present studies, we have determined that the ATP sites are not identical and are asymmetrically arranged in intact P-gp, which has led us to suggest an extension of this model to include the possibility that each hydrolysis event would subserve a different function depending on context. In CFTR, for instance, another member of the ABC transporter family, the two ATP sites are thought to perform different functions (21). Current estimations of the stoichiometry of ATP hydrolysis per drug transported by P-gp do not allow a distinction to be made between 1–3 mol of ATP hydrolyzed per drug molecule transported (54, 55). In P-gp, we would suggest that the second round of hydrolysis and the resultant release of ADP and phosphate may not serve to pump or release another drug molecule out of the cell but instead may serve to reset the transporter to its original state or serve in some way to complete the transport and extrusion of the molecule of drug that stimulated the first round of ATP hydrolysis.

REFERENCES

- Gottesman, M. M., Hrycyna, C. A., Schoenlein, P. V., Germann, U. A., and Pastan, I. (1995) *Annu. Rev. Genet.* 29, 607–649.
- Gottesman, M. M., and Pastan, I. (1993) *Annu. Rev. Biochem.* 62, 385–427.
- Chen, C.-j., Chin, J. E., Ueda, K., Clark, D. P., Pastan, I., Gottesman, M. M., and Roninson, I. B. (1986) *Cell* 47, 381–389.
- Gottesman, M. M., and Pastan, I. (1988) *J. Biol. Chem.* 263, 12163–12166.
- Hrycyna, C. A., Airan, L. E., Germann, U. A., Ambudkar, S. V., Pastan, I., and Gottesman, M. M. (1998) *Biochemistry* 37, 13660–13673.
- Raviv, Y., Pollard, H. B., Bruggemann, E. P., Pastan, I., and Gottesman, M. M. (1990) *J. Biol. Chem.* 265, 3975–3980.
- Higgins, C. F. (1992) *Annu. Rev. Cell Biol.* 8, 67–113.
- Walker, J. E., Saraste, M., Runswick, M. J., and Gay, N. J. (1982) *EMBO J.* 1, 945–951.
- Ames, G. F. (1986) *Annu. Rev. Biochem.* 55, 397–425.
- Hyde, S. C., Emsley, P., Hartshorn, M. J., Mimmack, M. M., Gileadi, U., Pearce, S. R., Gallagher, M. P., Gill, D. R., Hubbard, R. E., and Higgins, C. F. (1990) *Nature* 346, 362–365.
- Bakos, E., Klein, I., Welker, E., Szabo, K., Muller, M., Sarkadi, B., and Varadi, A. (1997) *Biochem. J.* 323, 777–783.
- Hoof, T., Demmer, A., Hadam, M. R., Riordan, J. R., and Tummler, B. (1994) *J. Biol. Chem.* 269, 20575–20583.
- Gottesman, M. M., Dey, S., Hrycyna, C. A., Ramachandra, M., Pastan, I., and Ambudkar, S. V. (1999) *Annu. Rev. Pharmacol. Toxicol.* 39, 361–398.
- Loo, T. W., and Clarke, D. M. (1995) *J. Biol. Chem.* 270, 21449–21452.
- Azzaria, M., Schurr, E., and Gros, P. (1989) *Mol. Cell. Biol.* 9, 5289–5297.

16. Muller, M., Bakos, E., Welker, E., Varadi, A., Germann, U. A., Gottesman, M. M., Morse, B. S., Roninson, I. B., and Sarkadi, B. (1996) *J. Biol. Chem.* 271, 1877–1883.
17. Urbatsch, I. L., Sankaran, B., Bhagat, S., and Senior, A. E. (1995) *J. Biol. Chem.* 270, 26956–26961.
18. Senior, A. E., al-Shawi, M. K., and Urbatsch, I. L. (1995) *FEBS Lett.* 377, 285–289.
19. Senior, A. E., and Bhagat, S. (1998) *Biochemistry* 37, 831–836.
20. Hrycyna, C. A., Ramachandra, M., Ambudkar, S. V., Ko, Y. H., Pedersen, P. L., Pastan, I., and Gottesman, M. M. (1998) *J. Biol. Chem.* 273, 16631–16634.
21. Gadsby, D. C., and Nairn, A. C. (1999) *Physiol. Rev.* 79, S77–S107.
22. Wu, Y. C., and Horvitz, H. R. (1998) *Cell* 93, 951–960.
23. Ramachandra, M., Ambudkar, S. V., Gottesman, M. M., Pastan, I., and Hrycyna, C. A. (1996) *Mol. Biol. Cell* 7, 1485–1498.
24. Jones, D. H., and Howard, B. H. (1990) *Biotechniques* 8, 178–183.
25. Pastan, I., Gottesman, M. M., Ueda, K., Lovelace, E., Rutherford, A. V., and Willingham, M. C. (1988) *Proc. Natl. Acad. Sci. U.S.A.* 85, 4486–4490.
26. Elroy-Stein, O., and Moss, B. (1991) in *Current Protocols in Molecular Biology* (Ausubel, F. M., Brent, R., Kingston, R. E., Moore, D. D., Smith, J. A., Seidman, J. C., and Struhl, K., Eds.) pp 16.19.1–16.19.9, John Wiley and Sons, New York.
27. Earl, P. E., Cooper, N., and Moss, B. (1991) in *Current Protocols in Molecular Biology* (Ausubel, F. M., Brent, R., Kingston, R. E., Moore, D. D., Smith, J. A., Seidman, J. C., and Struhl, K., Eds.) pp 16.16.1–16.16.7, John Wiley and Sons, New York.
28. Ramachandra, M., Gottesman, M. M., and Pastan, I. (1998) *Methods Enzymol.* 292, 441–455.
29. Ramachandra, M., Ambudkar, S. V., Chen, D., Hrycyna, C. A., Dey, S., Gottesman, M. M., and Pastan, I. (1998) *Biochemistry* 37, 5010–5019.
30. Hrycyna, C. A., Ramachandra, M., Pastan, I., and Gottesman, M. M. (1998) *Methods Enzymol.* 292, 456–473.
31. Hamada, H., and Tsuruo, T. (1986) *Proc. Natl. Acad. Sci. U.S.A.* 83, 7785–7789.
32. Georges, E., Bradley, G., Garipey, J., and Ling, V. (1990) *Proc. Natl. Acad. Sci. U.S.A.* 87, 152–156.
33. Bruggemann, E. P., Chaudhary, V., Gottesman, M. M., and Pastan, I. (1991) *Biotechniques* 10, 202–209.
34. Weber, J., Hammond, S. T., Wilke-Mounts, S., and Senior, A. E. (1998) *Biochemistry* 37, 608–614.
35. Hung, L. W., Wang, I. X., Nikaido, K., Liu, P. Q., Ames, G. F., and Kim, S. H. (1998) *Nature* 396, 703–707.
36. Hrycyna, C. A., Zhang, S., Ramachandra, M., Ni, B., Pastan, I., and Gottesman, M. M. (1996) in *Multidrug Resistance in Cancer Cells* (Gupta, S., and Tsuruo, T., Eds.) pp 29–37, John Wiley & Sons, Ltd., New York.
37. Beck, W. T., Mueller, T. J., and Tanzer, L. R. (1979) *Cancer Res.* 39, 2070–2076.
38. Germann, U. A., Willingham, M. C., Pastan, I., and Gottesman, M. M. (1990) *Biochemistry* 29, 2295–2303.
39. Schinkel, A. H., Kemp, S., Dolle, M., Rudenko, G., and Wagenaar, E. (1993) *J. Biol. Chem.* 268, 7474–7481.
40. Urbatsch, I. L., Beaudet, L., Carrier, I., and Gros, P. (1998) *Biochemistry* 37, 4592–4602.
41. Bruggemann, E. P., Germann, U. A., Gottesman, M. M., and Pastan, I. (1989) *J. Biol. Chem.* 264, 15483–15488.
42. Dey, S., Ramachandra, M., Pastan, I., Gottesman, M. M., and Ambudkar, S. V. (1997) *Proc. Natl. Acad. Sci. U.S.A.* 94, 10594–10599.
43. Urbatsch, I. L., Sankaran, B., Weber, J., and Senior, A. E. (1995) *J. Biol. Chem.* 270, 19383–19390.
44. Cremo, C. R., Long, G. T., and Grammer, J. C. (1990) *Biochemistry* 29, 7982–7990.
45. Mechetner, E. B., Schott, B., Morse, B. S., Stein, W. D., Druley, T., Davis, K. A., Tsuruo, T., and Roninson, I. B. (1997) *Proc. Natl. Acad. Sci. U.S.A.* 94, 12908–12913.
46. Arceci, R. J., Stieglitz, K., and Bierer, B. E. (1992) *Blood* 80, 1528–1536.
47. Sharom, F. J. (1995) *J. Bioenerg. Biomembr.* 27, 15–22.
48. Ambudkar, S. V., Lelong, I. H., Zhang, J., Cardarelli, C. O., Gottesman, M. M., and Pastan, I. (1992) *Proc. Natl. Acad. Sci. U.S.A.* 89, 8472–8476.
49. Georges, E., Zhang, J. T., and Ling, V. (1991) *J. Cell. Physiol.* 148, 479–484.
50. Al-Shawi, M. K., Urbatsch, I. L., and Senior, A. E. (1994) *J. Biol. Chem.* 269, 8986–8992.
51. Al-Shawi, M. K., and Senior, A. E. (1993) *J. Biol. Chem.* 268, 4197–4206.
52. Loo, T. W., and Clarke, D. M. (1995) *J. Biol. Chem.* 270, 22957–22961.
53. Senior, A. E., and Gadsby, D. C. (1997) *Semin. Cancer Biol.* 8, 143–150.
54. Shapiro, A. B., and Ling, V. (1998) *Eur. J. Biochem.* 254, 189–193.
55. Ambudkar, S. V., Cardarelli, C. O., Pashinsky, I., and Stein, W. D. (1997) *J. Biol. Chem.* 272, 21160–21166.

BI991115M